

FIRST EXPERIMENTS WITH CONVERGENT MULTI-IMAGES PHOTOGRAMMETRY WITH AUTOMATIC CORRELATION APPLIED TO DIFFERENTIAL RECTIFICATION OF ARCHITECTURAL FAÇADES

J. García-León^{a,*}, A. M. Felicísimo^a, J. J. Martínez^b

^a Ingeniería Cartográfica, Geodesia y Fotogrametría, Escuela Politécnica, Universidad de Extremadura, 10071 Cáceres, Spain - (jleon, amfeli)@unex.es

^b Expresión Gráfica Arquitectónica, Universidad Politécnica de Cartagena, 30202 Cartagena, Spain – juanjo.martinez@upct.es

Commission VI, WG VI/4

KEY WORDS: convergent multi-images, automatic correlation, DSM.

ABSTRACT:

In architectural photogrammetry, convergent geometry has some advantages over normal geometry. One of them is the reduction of the number of images needed for the full coverage of the object. This advantage simplifies network design and increases theoretically the accuracy of the method and internal reliability (Mason, 1994). However, the method has still not been widely used in practice because, probably the workflow has not been as consolidated as in the case of normal geometry.

In this article, we present and discuss the workflow to make a Digital Surface Model (DSM) of architectural façades semi-automatically and using convergent geometry. The accuracy of DSM is verified using an independent group of checkpoints, measured using conventional topographical methods. The influential parameters in the quality of DSM are discussed.

Finally, the influential factors are discussed and lines of development are proposed in order to overcome the present difficulties.

The results and discussion are based on a practical example using an historical monument in the medieval city of Cáceres (Spain), declared a World Heritage City in 1986.

1. INTRODUCTION

1.1 Approach to the problem

Architectural photogrammetry continues to be made with the strict limitations of aerial photogrammetry, in which the geometry is normal, the base is constant and the scale is uniform. These restrictions limit the flexibility now of recording data, increasing the number of images and requiring true acrobatics in order to resolve hidden areas. (See, for instance, Desmond & Bryan, 2001).

Changing the geometry and data processing strategies would solve part of the previously mentioned problems. This work presents a group of experiments in which the options chosen have been the following:

- The exposure is not normal but oblique and its geometry convergent.
- The overlapping is large, practically 100%.
- The images are multiple, up to 11 images.

There are three main reasons for this design:

- the oblique image solves the problems of space and camera movement.
- The number of images necessary for the complete coverage is less than in the case of normal geometry.

- The multiple images assure that there will be a repetition, which may be taken advantage of in order to obtain results that are more precise.

Data processing is the next problem since the photogrammetric applications are designed principally for the treatment of aerial case, with normal geometry (Patias & Tsioukas, 1999). In this case an application is needed which will allow work to be done with a multi-images convergent network and photogrammetry in addition to implementing algorithms of stereo-matching for automatic Digital Surface Models (DSM) generation. The only commercial application that contains these characteristics is the extension Orthobase Pro of Erdas Imagine extension. Orthobase Pro allows for the adjustment of multiple networks with oblique images specifically designed for terrestrial photogrammetry. There are object programs that allow adjustments to be made with these types of networks but they are not able to execute a completely automatic DSM and you can work only with an outside of an ensemble of points marked on the object (see, for instance, Otepka, et al, 2002)

1.2 Goals

Once the net and the computer applications were defined, the work focused on a principal objective: achievement of a DSM with a maximum density of points and the best precision possible. In order to carry this out, experiments were performed in which various value combinations were tested for a group of

* Corresponding author.

potentially influential variables. The results will allow for a discussion concerning aspects such as the adaptation of the software to the type of geometry, which factors can limit the DSM precision and possible improvements or corrections in order to advance in the automatic architectural generation of DSM.

2. MATERIAL AND DATA

2.1 Material

The photographs were done with Agfapan APX 100 Professional (Agfa, 100° ASA) and Technical Pan 6415 (Kodak, 25° ASA) film. A semi metric Rolleiflex 6008 with a 60 mm objective was used for the exposure. The negatives were digitalized with an UltraScan 5000 (Vexcel) scanner. The objective focal length was determined in relation to the space available in front of the façade. The two films were selected in order to check for possible differences due to different sensitivity and grain size.

The photogrammetric operations have been carried out with Erdas Imagine® 8.5 with OrthoBase Pro (Leica Geosystems). This application is the only commercial program that allows the adjustment of convergent images and the use of automatic stereo matching for DSM construction. The error calculus and subsequent analyses were carried out with the SIG ArcView 3.2a (ESRI) and the extensions with Spatial Analyst 2.0a and 3D Analyst 1.0.

2.2 Data

This work was carried out on one of the churches of the historical centre: San Mateo Church, sited in Cáceres (Western Spain, city declared World Heritage by UNESCO in 1986). The Southern façade has a complex design due to the presence of one tower and some relieves that frame the main gate. All these elements make this church ideal for our study (Figure1).



Figure 1. Southern façade of San Mateo Church.

3. METHODS

3.1 The taking and pre-processing of data

The taking and preparation of data can be divided into the following stages:

3.1.1 Geodetic network. The form and size of the signals were designed for an optimum recognition in relation to the characteristics exposure and digitisation. The point size is 31×31 mm, which corresponds approximately with a matrix of 17×17 pixels (see 3.1.3 and Figure 2).

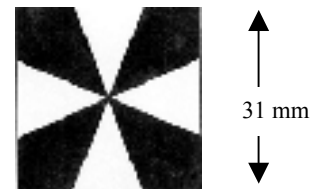


Figure 2. Signal designed for an oblique exposure.

The façade was marked with signals that determined the position of a total of 12 control points and 75 check points (Figure 3). The positioning of these points in the local system of coordinates was calculated through simple or multiple direct intersections with a reflectorless total station TCRM 1102plus (Leica Geosystems).

3.1.2 Photographic exposures and developing. The points of photographic exposures form a convergent network of 11 images. The central image is perpendicular to the façade and the rest of them are taken with an increment of 5° at both sides up to a maximum of 25° (Figure 4). From each point, two pictures were taken with the two films we are working with (APX 100 and Pan 6415).



Figure 3. Positioning of the control and check points on the façade.

The developing of the photographic film was carried out with the best products according to the manufacturer's

specifications: Agfa Rodinal and Kodak Technidol, the second one being specific for Technical Pan film.

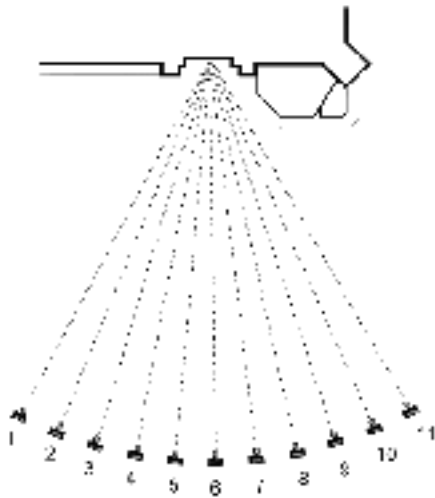


Figure 4. Design of the converging network.

3.1.3 Negative digitisation. The digitisation was done with the use of a Vexcel Ultrascan 5000 scanner with a pixel size of 5 μm . The pixel dimension was calculated in relation to the resolution of the APX 100 (150 lines/mm) film and the formula proposed by Kraus (1993). The size of the pixel represents approximately 1.8mm of the central area of the façade.

3.2 Photogrammetric process

The steps followed are the typical ones in the conventional photogrammetric process: internal and external orientation and DSM Construction. The difference in this case is that the Orthobase Pro allows a simultaneous adjustment of these 11 images.

The DSM construction is accomplished by automatic methods of stereo matching. However, Orthobase Pro cannot take advantage of the network as a whole and the models are constructed from only a pair of images. Thus, each combination of two images allows for a different DSM. The results are points that permit the construction of a Triangulated Irregular Network (TIN) structure (Peucker et al., 1978).

3.3 Error control

The error control was carried out by comparing the z coordinates (depth) out of the 75 checkpoints of the DSM (Figure 5). The results are expressed as Root Mean Square Error (RMSE). The DSM data for a concrete localization (x,y) is estimated through interpolation based on the TIN. Thus, it is interesting to have a dense TIN, formed by an elevated number of points. The contrary is equivalent to a process of generalization that would have foreseeable visible negative influences on the error statistics.

The control points will not always be available in their totality, since, according to the photographic pair, some may be in hidden areas. In this case, the points are eliminated before the error control is performed.



Figure 5. Distribution of the check points.

4. RESULTS

4.1 Adjustment error and network design

The internal orientations were adjusted with errors that were always inferior to the pixel (5 μm) size. The external orientations were adjusted with standard deviation values of 0.49 and 0.66 pixels. The calculation of the centres of projection had identical results with both films, with variations that never surpassed 9 mm with the exception of point 7 (14 mm). Network adjustments have been carried out from a minimum of three images up to a maximum of 11. The exactitude of the bundle adjustment was independent of the number of exposures included in the network. The standard deviation of the adjustment in the minor block (3 images) was of 0.48 pixels with 980 tie points. In the 11 image block, the standard deviation was of 0.49 pixels with 3400 tie points.

4.2 Stereo-matching Strategy

Although Orthobase Pro uses a “simplified structural matching” algorithm (Wang, 1998), it is not clear in which stages of the process this algorithm or other alternatives take part (Karras et al., 1998). The configuration process of stereo matching by the user can only be modified in minor factors: the selection of the search window sizes and their correlation. It should be noted that in epipolar images, the first of these factors might play a less important role. However, our tests reveal a surprising result that is detailed below.

The determination of the tie points is done automatically once the support points and the size of the search windows and correlation are defined. Apparently, the number of tie points that are recognized is determined by a threshold value of the correlation coefficient. The data associated to the tie points include information on two interesting characteristics: the number of images in which the point has been acknowledged and what those images are. Analyzing the reports, two facts may be determined: 1) most tie points are recognized in only two images and 2) these pairs are formed by images with the minimum convergence angle allowed by the block. When the network is formed by 11 images, the majority of the tie points are recognized in pairs with a convergence angle of 5°. When a network is formed, for example, by images 1-5-9 the tie points

are recognized in pairs 1-5 and 5-9, both of them with 20° of convergence.

These results suggest that the software could identify homologous points with large or moderate convergence angles but it is designed to use the smallest disposable angles in relation to the design of the network. This effect may be caused by the less good result obtained when a larger convergence angle is used (see 4.3.1). These results may be due to the different overlapping of the correlation windows on images taken with different angles of incidence. It ought to be considered that in this case the homologous points should be identified based on the textures of the façade. Other studies attempt to resolve these limitations through marking the object with a great number of signals (Edmundson & Baker, 2001). This strategy, in addition to being very laborious, cannot be applied to historic monuments.

4.3 DSM Precision

110 DSMs have been constructed (55 DSMs with each type of photographic film). These DSMs present different precisions according to some variables that have influence on the process. Experiments have been performed in order to check the effect of these variables and select the best possible combination to generate a DSM of greater precision. The variables analysed are the following:

4.3.1 Convergence angle. The precision of the DSM is conditioned by the convergence angle of the two images that make up the stereoscopic pair. In Figure 6 a collection of experiments is represented where it is proven that the error increases significantly with that angle:

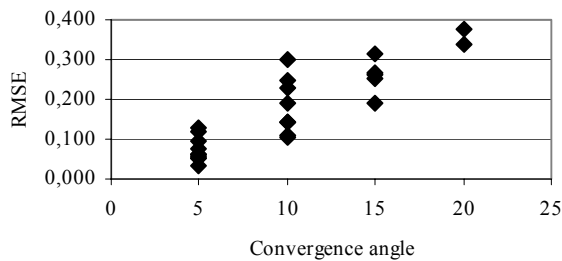


Figure 6. Relation between the convergence angle and the precision of the DSM expressed as RMSE in meters.

These results indicate the bad behaviour of the application even in moderately convergent exposures. This is in apparent contradiction with Wang's work (Erdas web page) where it is proven that the turns and distortions are not obstacles for a correct matching among the images. It also contradicts the theory of the convergent network configuration, whose optimum geometry is configured with angles from 60° to 90° (Mason, 1994). It is, however, in agreement with the results commented in section 4.2 where the recognition of homologous points is preferably achieved in neighbouring images with a convergence angle of 5°.

4.3.2 Size of the search windows and correlation. Tests have been accomplished to demonstrate that the size of the search window influences the number of points of the DSM. Different analyses were carried out fixing the coefficient values

of the threshold correlation (0.85) and the correlation window (7x7) but varying the size of the search window. The results demonstrate that the tie point number increases and the adjustment error descend if the search window is reduced.

4.3.3 Elimination of gross errors. There are two types of gross errors. The first one is due to errors in the identification of homologous points and is usual in any photogrammetric process. In our case, there is a second type of error derived from the existence of hidden areas in some of the images of the pair. The first type of error was reduced by examining the improvement in the precision of the DSM when the check points with the greater errors were eliminated.

When the improvement curve reaches an inflection point the DSM is considered to be purged of large errors. The highest value (0.122 m) corresponds to the whole sample. By eliminating the greatest error point, the RMSE descends to 0.105 m. The purging of gross errors finalized when the 5 points with the greatest errors are eliminated. At this point, the curve shows an inflection and the error slope is shallow. The values of the confidence interval were estimated according to the formula proposed by Li (1991). Figure 7 shows an example in which the RMSE value is related to the check points.

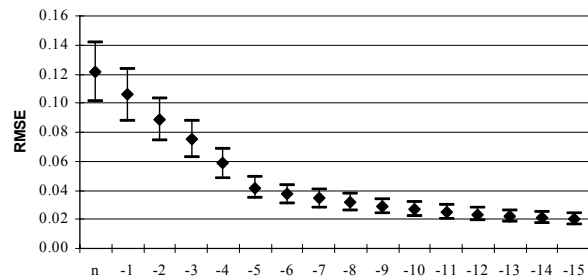


Figure 7. Improvement of the precision of the DSM with the elimination of the check points with the greater errors. The vertical strokes show the value of the confidence interval at the 95%.

The second kind of errors, derived from false correlations of hidden points, were eliminated using geometric criteria since it was already calculated which parts of the façade would be visible or not for each stereoscope pair.

4.3.4 DSM errors. Selecting the best values for the search and correlation windows and by eliminating gross errors, the DSMs are constructed for each pair of stereoscopes with a 5° convergence and for each type of film, which may influence in the contrast curves and grain size characteristic of each brand. The results demonstrate that the average RMSE value with Technical Pan (Kodak, 25° ASA) is slightly better than with Agfapan APX 100; the DSM present better precision values in seven out nine cases analysed. The results are shown in Table 1.

MDS (pair)	Film		
	Agfapan APX 100	Kodak Technical Pan	
		<i>all points</i>	<i>status = 1</i>
M1-2	0.055	0.044	0.031
M2-3	0.060	0.043	0.036
M3-4	0.031	0.055	0.033
M4-5	0.042	0.031	0.033
M6-7	0.025	0.016	0.016
M7-8	0.025	0.017	0.015
M8-9	0.030	0.010	0.009
M9-10	0.022	0.028	0.019
M10-11	0.034	0.023	0.020
Mean	0.036	0.030	0.023

Table 1. RMSE (m) values for the individual DSM and the average RMSE from the group for each type of film. The right column shows the improvement after the elimination of points with $r < 0.85$ (See 4.3.5).

Figure 8 shows a graphic representation of the DSM corresponding to the M1-2 (APX 100) pair. The grey tones respond to the depth value (z).



Figure 8. Example of DSM constructed with M1-2 (Pan) pair. There is an empty area (hidden) to the right of the tower.

4.3.5 Correlation coefficient value. For the detection of tie points, it is necessary to define a threshold value that works as a filter. In the construction of the DSM the possibility of selecting a threshold value does not exist. The result is formed by a group of points calculated with variable correlation values. The application assigns a value (“status”) to each point according to the correlation coefficient r : 1: $r \geq 0.85$; 2: $0.85 > r \geq 0.70$, 3: $0.70 > r \geq 0.50$. Status 4 (isolated) and 5 (suspicious) are not defined in relation to r .

The tests of error control show that the elimination of points with a worse correlation improves the results. Conserving the points with a status of one exclusively improvements are obtained in almost every case, especially in those that had

demonstrated worse precision (right column in Table 1). This test shows that the correlation coefficient may be used as an estimator of the data reliability.

4.4 Improvement: a synthesis DSM

It has already been indicated that the DSMs are constructed from a sole stereoscopic pair. Since the application does not construct a DSM by using all the data on the network, a synthesis has been carried out which follows the steps hereafter:

- Elimination of gross errors and hidden points in each DSM
- Elimination of all points with $status \neq 1$ (not optimum correlation)
- Union of individual DSMs
- Error control in the synthesis DSM

The results are clear: the synthesis DSM shows a better precision than the individual DSM. In this case, the film is a differential factor: the DSM constructed with Agfapan APX 100 is made up of 565926 points (RMSE = 0.020 m) while with Kodak Technical Pan 1057338 points are arrived at (RMSE = 0.015 m). That is, not only the error value improves at 25 %, but also the quantity of points is almost double with Technical Pan film. The improvement with respect to the group of DSM (Table 1) is important in both cases since the RMSE is reduced to half approximately.

4.5 Discussion

Convergent networks with multiple images still cannot be treated with maximum results using current commercial software. In the case of Orthobase Pro, it is possible to obtain adjustment statistics for a converging network but it is only possible to obtain DSM per image pair. The adjustments worsen with the convergence angle. This fact suggests that the converging network designs have not been used but that adaptations have been made with algorithms of normal geometry.

There is another evidence that indicates that the processes accomplished with Orthobase Pro are an “inheritance” from the standard aerial photogrammetry. For example, the Z-axis should be orientated towards the camera in order to carry out the DTM and it is obligatory that the façade be geo-referenced in regard to a projection system to fulfil the orthoimage.

The improvement methods of DSM should include the detection of blunders due to spurious correlations in hidden areas. The criteria could be purely zone-related before the division of the façade into visible/non-visible areas for each stereoscopic pair. The detection of other errors may be based on the definition of geometric constraints, at least in the façades that may be skeltonized into simple surfaces that may serve as a geometric reference or context.

The results improve through a selection of points based on the correlation coefficient. The union of the individual DSMs after an elimination of gross errors, hidden areas and poor points of correlation notably improves the result obtaining a DSM of a great quantity of points and a low error quantity. This may be the path to follow in order to take advantage of the possibilities of the software used.

The recognition of homologous points in images with different perspectives does not seem to be efficiently resolved. A greater effort becomes necessary in the design of efficient algorithms

adapted to exposures that are not normal. In the same way, the convergent networks possess a high degree of redundancy that must be used to generate a robust DSM.

Finally, it must be noted that DSM are not authentic three-dimensional models since the hidden areas (folds) may not be modelled. This is not excessively important for the construction of orthoimages but renders the construction of true 3D models impossible. The path towards this objective demands a deep revision of the algorithmic basis implemented in current photogrammetric applications.

4.6 References

Desmond, L.G., Bryan, P.G., 2001. Photogrammetric survey of the Adivino Pyramid at the Mayan archaeological site of Uxmal, Yucatan, Mexico. *Proceedings of the Seventh International Conference on Virtual Systems and Multimedia, V/SMM'01*. IEEE, Berkeley, California, October 25-27.

Edmundson, K., Baker, L., 2001. Photogrammetric measurement of the Arecibo primary reflector surface. *Proceedings of the Coordinate Measurement Systems Committee Conference*, CMSC, Albuquerque, New Mexico, August 13-17.

Karras, G.E., Mavrogenneas, N., Mavrommati, D., Tsikonis, N., 1998. Tests on Automatic DEM Generation in a Digital Photogrammetric Workstation. *International Archives of Photogrammetry and Remote Sensing*, 32(2), pp136-139.

Kraus, K., 1993. *Photogrammetry. Vol. 1. Fundamentals and Standard Processes*. Dümmler Verlag, Bonn, pp. 346-347.

Li, Z., 1991. Effects of checkpoints on the reliability of DTM accuracy estimates obtained from experimental tests. *Photogrammetric Engineering & Remote Sensing*, 57(10), pp. 1333-1340.

Mason, S.O., 1994. *Expert system-based design of photogrammetric networks*. Dissertation ETH Nr. 10475. Institute for Geodesy and Photogrammetry, Swiss Federal Institute of Technology (EYH), p.50.

Otepka, J.O., Hanley, H.B., Fraser, C.S., 2002, Algorithm developments for automated off-line vision metrology. *Proceedings of the ISPRS Commission V Symposium*, ISPRS, Corfu, Greece, September 1-2, pp. 60-67.

Patias, P., Tsioukas, V. 1999. Multi-Image Matching for Architectural and Archaeological Orthoimage Production. *Proceedings of XVII CIPA Symposium*, Olinda, Brazil, printed in symposium CD.

Peucker, T.K., Fowler, R.J., Little, J.J. & Mark, D.M., 1978. The triangulated irregular network. *Proceedings of the ASP Digital Terrain Models (DTM) Symposium*, American Society of Photogrammetry, Sant Louis, Missouri, May 9-11, pp. 516-540.

Wang, Y., 1998. Principles and applications of structural image matching. *ISPRS Journal of Photogrammetry and Remote Sensing*, 53, pp. 154-165.

Wang, Y. (Erdas web page) Fully automatic image matching. Digital image matching with structural matching techniques, 3

p. Geosystems GmbH. <http://www.geosystems.de/produkte/orthobase.html> (accessed 12 June 2003).

4.7 Acknowledgements

To ESRI España and Leica Geosystems for the granting of temporary Erdas Imagine licences for the carrying out of this work. To the Junta de Extremadura for their collaboration.